ECCOMAS Congress 2016
VII European Congress on Computational Methods in Applied Sciences and Engineering
M. Papadrakakis, V. Papadopoulos, G. Stefanou, V. Plevris (eds.)
Crete Island, Greece, 5–10 June 2016

ADAPTIVE BEM-BASED FEM ON POLYGONAL MESHES FROM VIRTUAL ELEMENT METHODS

S. Weißer

Saarland University
Campus building E1.1, 66041 Saarbrücken, Germany
weisser@num.uni-sb.de

Keywords: BEM-based FEM, polygonal meshes, residual based error estimate, adaptivity

Abstract. *Polygonal meshes are especially suited for the discretization of boundary value problems in adaptive mesh refinement strategies. Such meshes are very flexible and incorporate hanging nodes naturally. But only a few approaches are available that handle polygonal discretizations in this context. The BEM-based Finite Element Method (FEM) and a residual based error estimate are reviewed in the presentation. This a posteriori error estimate is reliable and efficient on polygonal meshes and can be applied in adaptive FEM strategies. Furthermore, the BEM-based FEM is applicable on such general meshes and gains its flexibility by implicitly defined trial functions. They are given as solutions of local Dirichlet problems related to the global differential operator. These local problems are treated by means of Boundary Element Methods (BEM) in the realization. In the numerical experiments the test problems of the recent publication on adaptive Virtual Element Methods by L. Beirão da Veiga and G. Manzini [ESAIM Math. Model. Numer. Anal., 49(2):577–599, 2015] are considered in an adaptive BEM-based FEM simulation. The experiments show optimal rates of convergence for uniform and adaptive mesh refinement, where the latter one yields, in particular, very local mesh adaptation.*

1 Introduction

Polygonal and polyhedral meshes have attracted a lot of interest in the discretization of boundary value problems during the last few years. Especially in adaptive mesh refinement strategies such meshes are attractive, since they are very flexible and handle hanging nodes naturally. New methods have been developed and conventional approaches were mathematically revised to handle these general meshes. The most prominent representatives for the new approaches are the Virtual Element Method (VEM) [2] and the Weak Galerkin Method [17]. Strategies like discontinuous Galerkin [7] and the mimetic discretization techniques [3] are also considered on polygonal and polyhedral meshes. Additionally, there are the so called BEM-based Finite Element Methods (FEM) which have their roots in the boundary element domain decomposition approaches [6]. These methods make use of implicitly defined trial functions that are locally the solution of boundary value problems treated in the numerical realization by means of Boundary Element Methods (BEM).

The BEM-based FEM has been studied for high order approximations [13, 20], mixed formulations [9], convection-adapted trial functions [10], time dependent problems [21] and on general polyhedral meshes [14]. Additionally, the BEM-based FEM has shown its flexibility and applicability on adaptively refined polygonal meshes [18, 22, 23]. Especially adaptivity is an interesting topic in this context, but, there are only a few references to adaptive strategies and a posteriori error control on polygonal meshes. A posteriori error estimates for the discontinuous Galerkin method are given in [11]. To the best of our knowledge there is only one publication for the Virtual Element Method [4] and one for the Weak Galerkin Method [5]. The first mentioned publication deals with a residual a posteriori error estimate for a C^1-conforming approximation space, and the second one is limited to simplicial meshes. For the mimetic discretization technique there are also only few references which are limited to low order methods, see the recent work [1].

The aim of this publication is to review the findings for the adaptive BEM-based FEM and to present computational results obtained by the considered approach for the test problems studied in [4] for the Virtual Element Method. Beside of the high flexibility of the polygonal meshes, the numerical experiments show optimal rates of convergence on very locally adapted meshes. This is possible since no additional refinement in the neighbourhood of marked elements is necessary to keep the meshes admissible.

In Section 2, we give a model problem and discuss the preliminaries for the BEM-based FEM. The discretization is reviewed in Section 3, and in Section 4, the reliability as well as the efficiency of the residual based error estimate on polygonal meshes is stated. Section 5 describes the adaptive BEM-based FEM strategy and presents several numerical experiments. Finally, we give a conclusion in Section 6.

2 Preliminaries

Let $\Omega \subset \mathbb{R}^2$ be a connected, bounded, polygonal domain with unit outer normal field n_Ω. Furthermore, denote by $\Gamma = \Gamma_D \cup \Gamma_N$ the boundary of Ω, where $\Gamma_D \cap \Gamma_N = \emptyset$ and $|\Gamma_D| > 0$. We consider the diffusion equation with mixed boundary conditions

$$-\mathrm{div}(a\nabla u) = f \quad \text{in } \Omega, \qquad u = 0 \quad \text{on } \Gamma_D, \qquad a\nabla u \cdot n_\Omega = g_N \quad \text{on } \Gamma_N, \tag{1}$$

where, for simplicity, we restrict ourselves to piecewise constant and scalar valued diffusion $a \in L_\infty(\Omega)$ with $0 < a_{\min} \leq a \leq a_{\max}$ almost everywhere in Ω. The usual notation for Sobolev spaces and their norms is used.

The well known variational formulation of problem (1) reads

$$\text{Find } u \in H^1_D(\Omega): \quad b(u,v) = (f,v)_{L_2(\Omega)} + (g_N, v)_{L_2(\Gamma_N)} \quad \forall v \in H^1_D(\Omega), \tag{2}$$

for $g_N \in L_2(\Gamma_N)$ and $f \in L_2(\Omega)$, where

$$b(u,v) = (a\nabla u, \nabla v)_{L_2(\Omega)}$$

is bounded and coercive on

$$H^1_D(\Omega) = \{v \in H^1(\Omega) : v = 0 \text{ on } \Gamma_D\}.$$

We decompose the domain Ω into a family of meshes $\mathcal{K}_h$ containing non-overlapping, polygonal elements $K \in \mathcal{K}_h$ such that

$$\overline{\Omega} = \bigcup \{x \in \overline{K} \,\big|\, K \in \mathcal{K}_h\}.$$

The mesh is called regular if all elements $K \in \mathcal{K}_h$ are star-shaped with respect to a circle of radius ρ_K such that the ratio of the element diameter h_K and ρ_K is uniformly bounded, i.e. $h_K/\rho_K < \sigma_{\mathcal{K}}$, and if the element diameter can be uniformly bounded by a constant times the smallest length of its edges, i.e. $h_K < c_{\mathcal{K}} h_E$ for $E \in \mathcal{E}(K)$. Here, $\mathcal{E}(K)$ denotes the set of edges of K. Furthermore, we denote by $\mathcal{N}_h$ and $\mathcal{E}_h$ the sets of all nodes and edges in the mesh. $\mathcal{E}_h$ is decomposed into the sets of edges which are in the interior of Ω, on the Dirichlet boundary Γ_D and on the Neumann boundary Γ_N, we write $\mathcal{E}_h = \mathcal{E}_{h,\Omega} \cup \mathcal{E}_{h,D} \cup \mathcal{E}_{h,N}$. Additionally, we assume without loss of generality that $h_K < 1$, $K \in \mathcal{K}_h$. This is always achievable by scaling the domain.

Finally, the conforming approximation space $V_h^k \subset H^1_D(\Omega)$ of order k with

$$V_h^k = \{v \in H^1_D(\Omega) : \Delta v|_K \in \mathcal{P}^{k-2}(K), K \in \mathcal{K}_h \text{ and } v|_E \in \mathcal{P}^k(E), E \in \mathcal{E}_h\}$$

is introduced. Here $\mathcal{P}^p(\cdot)$ denotes the space of polynomials of degree smaller or equal p over the elements and edges, respectively. In the case of the diffusion equation, which is studied here, the approximation space V_h^k for the BEM-based FEM is the same as for the Virtual Element Method. But, in contrast to the Virtual Element Method, the BEM-based FEM makes use of an explicit basis of V_h^k.

3 BEM-based FEM

The discrete space V_h^k is constructed by prescribing its basis functions that are subdivided into nodal, edge and element basis functions. Each of them is locally (element-wise) the unique solution of a boundary value problem. We give a brief review of the approach in [20], more details concerning the implementation can also be found in [13].

For each node we define the function ψ_z, $z \in \mathcal{N}_h$ such that

$$-\Delta\psi_z = 0 \quad \text{in } K \quad \text{for all } K \in \mathcal{K}_h,$$

$$\psi_z(x) = \begin{cases} 1 & \text{for } x = z, \\ 0 & \text{for } x \in \mathcal{N}_h \setminus \{z\}, \end{cases}$$

ψ_z is linear on each edge of the mesh.

For $E \in \mathcal{E}_h$, let $z_0, z_1 \in \mathcal{N}_h$ with $E = \overline{z_0 z_1}$. We set $p_{E,0} = \psi_{z_0}|_E$ and $p_{E,1} = \psi_{z_1}|_E$. Furthermore, let $\{p_{E,i} : i = 0, \dots, k\}$ be a basis of $\mathcal{P}^k(E)$. Then the edge basis functions $\psi_{E,i}$ for $i = 2, \dots, k$, $E \in \mathcal{E}_h$ are given by

$$\begin{aligned} -\Delta \psi_{E,i} &= 0 \quad \text{in } K \quad \text{for all } K \in \mathcal{K}_h, \\ \psi_{E,i} &= \begin{cases} p_{E,i} & \text{on } E, \\ 0 & \text{on } \mathcal{E}_h \setminus \{E\}. \end{cases} \end{aligned}$$

Last but not least, we have to incorporate the non-harmonic functions. Consequently, we define the element basis functions $\psi_{K,i,j}$ for $i = 0, \dots, k-2$ and $j = 0, \dots, i$, $K \in \mathcal{K}_h$ by

$$\begin{aligned} -\Delta \psi_{K,i,j} &= p_{K,i,j} \quad \text{in } K, \\ \psi_{K,i,j} &= 0 \qquad \text{else}, \end{aligned}$$

where $\{p_{K,i,j} : i = 0, \dots, k-2 \text{ and } j = 0, \dots, i\}$ is a basis of $\mathcal{P}^{k-2}(K)$.

All these functions are well defined. They are given locally as unique solutions of a boundary value problems and, due to the local Dirichlet boundary data, they are continuous over the whole domain Ω. It is easily seen that $\{\psi_z, \psi_{E,i}, \psi_{K,i,j}\}$ forms a basis of V_h^k, since each function $\psi \in V_h^k$ can be expressed locally as solution of the boundary value problem

$$\begin{aligned} -\Delta \psi &= p_K \quad \text{in } K, \\ \psi &= p_{\partial K} \quad \text{on } \partial K, \end{aligned} \tag{3}$$

with $p_K \in \mathcal{P}^{k-2}(K)$ and $p_{\partial K} \in \mathcal{P}^k_{\mathrm{pw}}(\partial K)$. Here, $\mathcal{P}^k_{\mathrm{pw}}(\partial K) = \mathcal{P}^k_{\mathrm{pw,d}}(\partial K) \cap C^0(\partial K)$ and

$$\mathcal{P}^k_{\mathrm{pw,d}}(\partial K) = \{p \in L_2(\partial K) : p|_E \in \mathcal{P}^k(E), E \in \mathcal{E}(K)\}.$$

The Galerkin approximation of (2) reads

$$\text{Find } u_h \in V_h^k : \quad b(u_h, v_h) = (f, v_h)_{L_2(\Omega)} + (g_N, v_h)_{L_2(\Gamma_N)} \quad \forall v_h \in V_h^k. \tag{4}$$

For $\psi \in V_h^k$, $v \in H^1_D(\Omega)$ and $a(\cdot) = a_K$ on each $K \in \mathcal{K}_h$, it is

$$b(\psi, v) = \sum_{K \in \mathcal{K}_h} a_K (\nabla \psi, \nabla v)_{L_2(K)} = \sum_{K \in \mathcal{K}_h} a_K \left\{ (\gamma_1^K \psi, \gamma_0^K v)_{L_2(\partial K)} - (\Delta \psi, v)_{L_2(K)} \right\},$$

where $\gamma_0^K v$ is the usual trace of v on ∂K and $\gamma_1^K \psi \in H^{-1/2}(\partial K)$ is the Neumann trace of ψ on ∂K, which is given for sufficient regular ψ by

$$\gamma_1^K \psi(x) = \lim_{K \ni \tilde{x} \to x} n_K(x) \cdot \nabla \psi(\tilde{x}) \quad \text{for } x \in \partial K.$$

Since the Neumann trace is unknown in general, we approximate $\gamma_1^K \psi$ by $\widetilde{\gamma_1^K \psi} \in \mathcal{P}^k_{\mathrm{pw,d}}(\partial K)$ using a Galerkin approximation for a boundary integral equation connecting the Dirichlet and Neumann trace. If ψ is given by (3) with $p_K = 0$, that is always achievable by homogenization with a polynomial, the utilized formulation of the Boundary Element Method (BEM) reads:

$$\text{Find } \widetilde{\gamma_1^K \psi} \in \mathcal{P}^k_{\mathrm{pw,d}}(\partial K) : \ \left(\mathbf{V}_K \widetilde{\gamma_1^K \psi}, q \right)_{L_2(\partial K)} = \left(\left(\tfrac{1}{2} \mathbf{I} + \mathbf{K}_K \right) p_{\partial K}, q \right)_{L_2(\partial K)} \ \forall q \in \mathcal{P}^{k-1}_{\mathrm{pw,d}}(\partial K).$$

This formulation involves the single layer potential $\mathbf{V}_K : H^{-1/2}(\partial K) \to H^{1/2}(\partial K)$ and the double layer potential $\mathbf{K}_K : H^{1/2}(\partial K) \to H^{1/2}(\partial K)$, which are boundary integral operators. Thus, the task to find an approximation of the Neumann trace is reduced to a one-dimensional problem on the boundary ∂K. Furthermore, we have the representation formula

$$\psi(x) = \int_{\partial K} U^*(x,y)\gamma_1^K\psi(y)\,ds_y - \int_{\partial K} \gamma_{1,y}^K U^*(x,y)\gamma_0^K\psi(y)\,ds_y \quad \text{for } x \in K, \tag{5}$$

where $U^*(x,y) = -\frac{1}{2\pi}\ln(|x-y|)$. More details can be found in the literature on boundary integral equations and Boundary Element Methods, see, e.g., [12, 15].

Next, an approximation to the variational formulation (4) is given. Let $\widetilde{v}$ be a piecewise polynomial and discontinuous approximation of $v \in H_D^1(\Omega)$ over the mesh $\mathcal{K}_h$, which is obtained by local averaging for example. As proposed in [22], the approximated discrete variational formulation is defined by

$$\text{Find } u_h \in V_h^k: \quad b_h(u_h, v_h) = (f, \widetilde{v}_h)_{L_2(\Omega)} + (g_N, v_h)_{L_2(\Gamma_N)} \quad \forall v_h \in V_h^k, \tag{6}$$

with

$$b_h(\psi, v) = \sum_{K\in\mathcal{K}_h} a_K \left\{ (\widetilde{\gamma_1^K\psi}, \gamma_0^K v)_{L_2(\partial K)} - (\Delta\psi, \widetilde{v})_{L_2(K)} \right\}, \quad \psi \in V_h^k, v \in H_D^1(\Omega),$$

where $\widetilde{\gamma_1^K\psi} \in \mathcal{P}_{\mathrm{pw,d}}^{k-1}(\partial K)$ is the BEM approximation and $\widetilde{v}$ is the polynomial approximation of v over each K. This form of the approximated bilinear form is especially suited for the a-posteriori error analysis since the second argument of $b_h(\cdot,\cdot)$ is only assumed to be in $H_D^1(\Omega)$. For the computational realization one might exploit the additional properties of $v_h \in V_h^k$ to treat the volume integral $(\Delta\psi, \widetilde{v}_h)_{L_2(K)}$, see [13, 20].

4 Residual based Error Estimate

In this section, the residual based error estimate is reviewed on polygonal meshes and the reliability as well as the efficiency are stated. This estimate bounds the error of the finite element computation in the energy norm, which is given by $\|v\|_{b,\omega}^2 = (a\nabla v, \nabla v)_{L_2(\omega)}$ over a subset $\omega \subset \Omega$. Due to the homogenious Dirichlet boundary data, $\|\cdot\|_{b,\Omega}$ is equivalent to $\|\cdot\|_{H^1(\Omega)}$ on $H_D^1(\Omega)$. The discrete jump of the approximation of the conormal derivatives over an internal edge $E \in \mathcal{E}_{h,\Omega}$ is defined by

$$[\![u_h]\!]_{E,h} = a_K\widetilde{\gamma_1^K u_h} + a_{K'}\widetilde{\gamma_1^{K'} u_h},$$

where $K, K' \in \mathcal{K}_h$ are the adjacent elements of E with $E \in \mathcal{E}(K) \cap \mathcal{E}(K')$.

Theorem 1 (Reliability)**.** *Let $\mathcal{K}_h$ be a regular mesh. Furthermore, let $u \in H_D^1(\Omega)$ and $u_h \in V_h^k$ be the solutions of* (2) *and* (6)*, respectively. Then, it is*

$$\|u - u_h\|_{b,\Omega} \le c\,\left\{\eta_R^2 + \delta_R^2\right\}^{1/2} \quad \textit{with} \quad \eta_R^2 = \sum_{K\in\mathcal{K}_h}\eta_K^2 \quad \textit{and} \quad \delta_R^2 = \sum_{K\in\mathcal{K}_h}\delta_K^2,$$

where the error indicators are defined by

$$\eta_K^2 = h_K^2\|R_K\|_{L_2(K)}^2 + \sum_{E\in\mathcal{E}(K)} h_E\|R_E\|_{L_2(E)}^2, \qquad \delta_K^2 = \|a_K\gamma_1^K u_h - a_K\widetilde{\gamma_1^K u_h}\|_{L_2(\partial K)}^2,$$

with the element residual

$$R_K = f + a_K \Delta u_h \quad \textit{for } K \in \mathcal{K}_h,$$

and the edge residual

$$R_E = \begin{cases} 0 & \textit{for } E \in \mathcal{E}_{h,D}, \\ g_N - a_K \widetilde{\gamma_1^K u_h} & \textit{for } E \in \mathcal{E}_{h,N} \textit{ with } E \in \mathcal{E}(K), \\ -\frac{1}{2}[\![u_h]\!]_{E,h} & \textit{for } E \in \mathcal{E}_{h,\Omega}. \end{cases}$$

The constant $c > 0$ only depends on the regularity parameters $\sigma_{\mathcal{K}}$, $c_{\mathcal{K}}$, the approximation order k and on the diffusion coefficient a.

The term δ_K measures the approximation error in the Neumann traces of the basis functions of V_h^k coming from the Boundary Element Method. To state the efficiency, we introduce the neighbourhood ω_K of an element $K \in \mathcal{K}_h$. Let ω_K be an open subset of Ω such that

$$\overline{\omega}_K = \bigcup \{x \in \overline{K'} : \mathcal{E}(K) \cap \mathcal{E}(K') \neq \emptyset, K' \in \mathcal{K}_h\}.$$

Theorem 2 (Efficiency)**.** *Under the assumptions of Theorem 1, the following local bound is fulfilled*

$$\begin{aligned} \eta_K \;\leq\; c \Bigg(& \|u - u_h\|_{b,\omega_K}^2 + h_K^2 \|f - \widetilde{f}\|_{L_2(\omega_K)}^2 + \sum_{E \in \mathcal{E}(K) \cap \mathcal{E}_{h,N}} h_E \|g_N - \widetilde{g}_N\|_{L_2(E)}^2 \\ & + \sum_{E \in \mathcal{E}(K)} \sum_{K' \subset \omega_E} h_E \|a_{K'} \gamma_1^{K'} u_h - a_{K'} \widetilde{\gamma_1^{K'} u_h}\|_{L_2(E)}^2 \Bigg)^{1/2}, \end{aligned}$$

where $\widetilde{f}$ and $\widetilde{g}_N$ are piecewise polynomial approximations of the data f and g_N, respectively. The constant $c > 0$ only depends on the regularity parameters $\sigma_{\mathcal{K}}$, $c_{\mathcal{K}}$, the approximation order k and on the diffusion coefficient a.

The terms involving the data approximation $\|f - \widetilde{f}\|_{L_2(\omega_K)}$ and $\|g_N - \widetilde{g}_N\|_{L_2(E)}$ are often called data oscillations. They are usually of higher order. Furthermore, the approximation of the Neumann traces by the Boundary Element Method appear in the right hand side. This term is related to δ_K.

5 Numerical experiments

For the numerical validation and verification, we consider the two test cases given in [4] for an adaptive Virtual Element Method (VEM). The boundary value problems are given on bounded polygonal domains Ω as

$$-\Delta u = f \quad \text{in } \Omega, \qquad u = g_D \quad \text{on } \Gamma_D = \partial\Omega. \tag{7}$$

The Dirichlet data $g_D \in C(\Gamma_D)$ is treated in the usual way by a discrete extension into the domain Ω to obtain homogeneous data on Γ_D. Therefore, problem (7) takes the form (1). In the following, (7) is approximated on a sequence of uniformly and adaptively refined meshes, where the initial meshes coincide with the ones in [4]. For the refinement itself we chose a different procedure than in [4], namely the algorithm from [18].

In the uniform refinement strategy each element of the mesh is split into two new elements to obtain the next finer mesh. This splitting process is performed as described below. For the adaptive BEM-based FEM, we proceed in a common strategy, which involves a loop over the following four steps:

SOLVE The boundary value problem (1) is approximated by means of the BEM-based FEM on the current polygonal mesh using the approximation space V_h^k.

ESTIMATE The residual based error estimator η_R as well as the indicators η_K discussed in Section 4 are computed over each element of the discretization $\mathcal{K}_h$.

MARK A minimal subset $\mathcal{M}_h \subset \mathcal{K}_h$ of all elements are marked according to Dörflers strategy [8] such that

$$\left(\sum_{K \in \mathcal{M}_h} \eta_K^2 \right)^{1/2} \geq (1-\theta)\, \eta_R,$$

where $0 \leq \theta < 1$ is a user defined parameter. To obtain a minimal set $\mathcal{M}_h$, it is possible to sort the elements according to their indicators η_K and mark those with the largest indicators. Instead of that, we implemented the marking algorithm given in [8] to achieve linear complexity. Furthermore, we choose $\theta = 0.5$ in the numerical experiments.

REFINE Each marked element is refined and we consequently obtain a new mesh for the next cycle in the loop. For the refinement of an element K, we bisect K through its barycenter $\bar{x}$ orthogonal to its characteristic direction that is given as eigenvector to the largest eigenvalue of the matrix

$$M_{\text{Cov}} = \int_K (x-\bar{x})(x-\bar{x})^\top dx, \qquad \bar{x} = \frac{1}{|K|} \int_K x\, dx.$$

For more details see [18, 19]. Furthermore, we check the regularity of the mesh and refine additional elements if the condition $h_K < c_{\mathcal{K}} h_E$ for $E \in \mathcal{E}(K)$ is violated with a user defined parameter $c_{\mathcal{K}}$.

The adaptive mesh refinement process is kept very local. Only the marked and degenerated elements are bisected during the refinement. It is not necessary to resolve hanging nodes and keep the mesh admissible as for example in the *red-blue-green* refinement procedure for triangular meshes, see [16]. This advantage is due to the polygonal meshes with very flexible elements. The local refinement character can be seen in the following test problems in the Figures 1 and 3.

To analyse the experiments, we compute the relative error in the energy norm over each mesh in the convergence process. In contrast to the Virtual Element Method, it is possible to evaluate the approximation u_h inside of the elements by means of the representation formula (5). Therefore, we approximate $\|u - u_h\|_{b,\Omega}$ by Gaussian quadrature over a fine auxiliary triangulation of the domain that is aligned with the polygonal mesh. The mesh size $h_{\max} = \max\{h_K : K \in \mathcal{K}_h\}$ does not uniformly tend to zero on adaptively refined meshes. Thus, the relative errors $\|u-u_h\|_{b,\Omega}/\|u\|_{b,\Omega}$ are plotted with respect to the number of degrees of freedom (DoF) in logarithmic scale. Since $\mathrm{DoF} = \mathcal{O}(h_{\max}^{-2})$ for a sequence of uniformly refined meshes, we expect that the error in the energy norm behaves like $\mathcal{O}(\mathrm{DoF}^{-k/2})$ for an optimal method with approximation order k.

5.1 Test case 1: singular solution

Let $\Omega = ((-1,1)\times(-1,1)) \setminus ([0,1]\times[-1,0])$ be a L-shaped domain and $f = 0$ in (7). The Dirichlet data g_D is chosen such that

$$u(r\cos\varphi, r\sin\varphi) = r^{2/3} \sin\left(\tfrac{2}{3}\varphi\right), \quad x = (r\cos\varphi, r\sin\varphi) \in \mathbb{R}^2$$

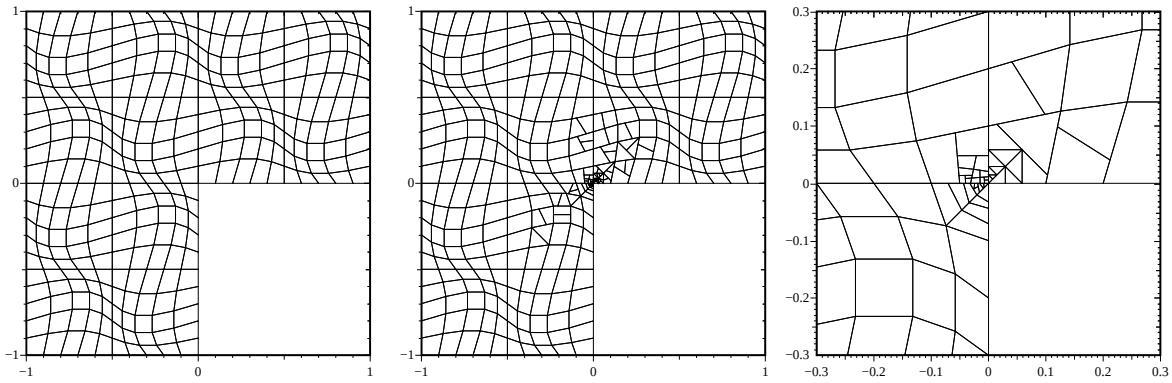

Figure 1: Test 1: initial mesh (left), adaptively refined mesh for $k = 1$ and $\|u - u_h\|_{b,\Omega}/\|u\|_{b,\Omega} \approx 0.02$ (middle), zoom of adaptively refined mesh for $k = 3$ and $\|u - u_h\|_{b,\Omega}/\|u\|_{b,\Omega} \approx 0.002$ (right).

is the exact solution of (7), where (r, φ) are polar coordinates. The initial mesh is visualized in Figure 1 (left). Furthermore, the adaptive refined meshes are given in this figure for the first order method with V_h^1 and a relative error of approximately 0.02 as well as for the third order method with V_h^3 and a relative error of approximately 0.002. In the right most picture a zoom of the mesh for V_h^3 is visualized since the adaptive refinement only affect elements close to the reentrant corner of the domain, where the singularity of the solution is located. The presented meshes were achieved after 11 and 16 refinement steps.

In Figure 2, the convergence graphs are given for the first, second and third order method and for the uniform as well as the adaptive strategy. In all three cases the adaptive BEM-based FEM yields optimal rates of convergence, namely a slope of $-k/2$ in the logarithmic plots. Since $u \in H^{5/3}(\Omega)$ is not sufficient regular, the convergence on uniform meshes slows down. The theory predicts a behaviour of the error independent of the approximation order k like $\mathcal{O}(h_{\max}^{2/3})$. This corresponds to $\mathcal{O}(\mathrm{DoF}^{-1/3})$, which is recovered in the convergence graphs in Figure 2.

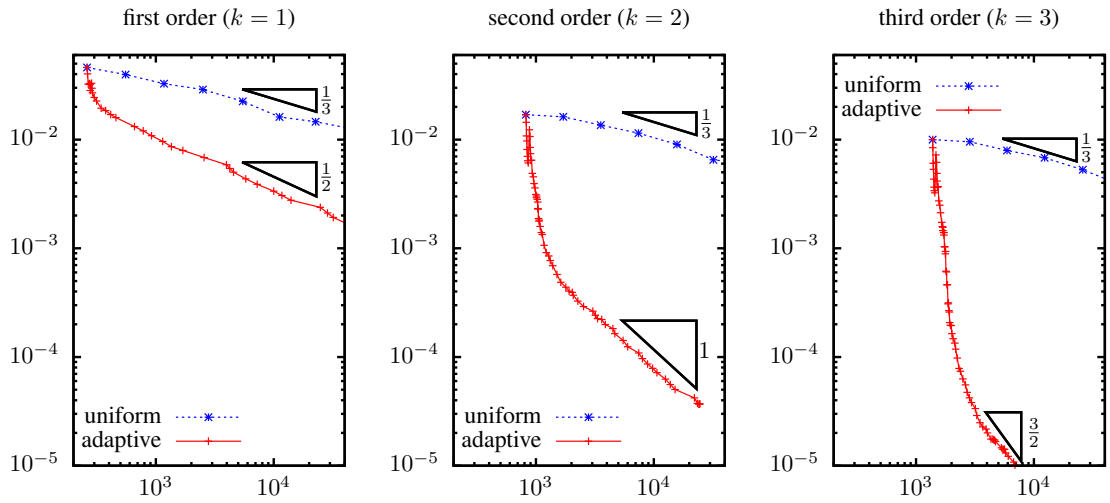

Figure 2: Test 1: convergence of the relative energy error $\|u - u_h\|_{b,\Omega}/\|u\|_{b,\Omega}$ with respect to the number of degrees of freedom for the approximation orders $k = 1, 2, 3$ on uniformly and adaptively refined meshes.

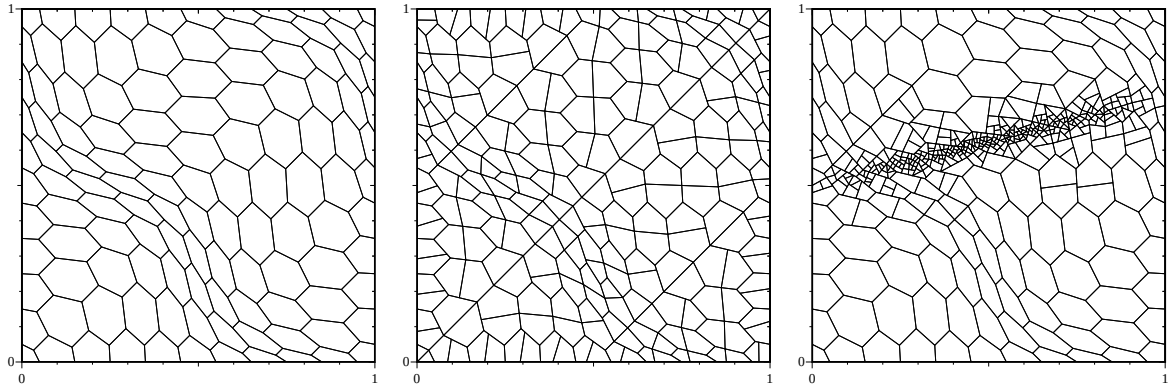

Figure 3: Test 2: initial mesh (left), uniformly refined mesh (middle), adaptively refined mesh for $k = 1$ and $\|u - u_h\|_{b,\Omega}/\|u\|_{b,\Omega} \approx 0.2$ (right).

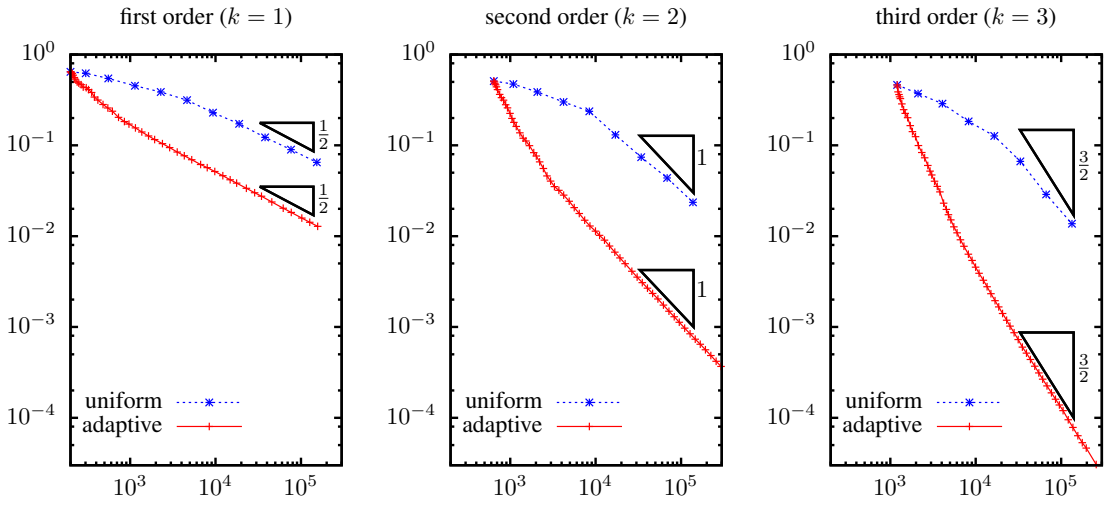

Figure 4: Test 2: convergence of the relative energy error $\|u - u_h\|_{b,\Omega}/\|u\|_{b,\Omega}$ with respect to the number of degrees of freedom for the approximation orders $k = 1, 2, 3$ on uniformly and adaptively refined meshes.

5.2 Test case 2: strong internal layer

Let $\Omega = (0, 1)^2$, $g_D = 0$ and f be chosen such that

$$u(x) = 16x_1(1 - x_1)x_2(1 - x_2)\arctan(25x_1 - 100x_2 + 50), \quad x = (x_1, x_2) \in \mathbb{R}^2$$

is the exact solution of (7). Since u is arbitrary smooth, we expect optimal rates of convergence in the case of uniform mesh refinement in an asymptotic regime. Although the solution u is smooth, it has a strong internal layer along the line $x_2 = 1/2 + x_1/4$. The initial mesh is visualized in Figure 3 (left). Furthermore, the first uniform refined mesh is given in the middle of Figure 3. Here, one recognizes that each polygonal cell is bisected in the refinement process. In the right most picture of Figure 3 the adaptively refined mesh for V_h^1 and a relative error of approximately 0.2 is presented. This mesh was achieved after 19 refinement steps. It is seen that the adaptive strategy refines along the internal layer of the exact solution.

In Figure 4, we give the convergence graphs for the first, second and third order method and for the uniform as well as the adaptive strategy. In all cases we recover the optimal convergence

rates which correspond to a slope of $-k/2$. But, for the uniform refinement, the internal layer has to be resolved sufficiently before the optimal rates are achieved. Since the adaptive strategy resolves the layer automatically, the adaptive BEM-based FEM is much more accurate for the same number of unknowns.

6 Conclusion

The numerical experiments have shown that polygonal meshes are appealing in adaptive FEM strategies. Their natural incorporation of hanging nodes allows very local mesh adaptations and facilitates the refinement process. The possibility to evaluate the approximation u_h inside of the elements in the BEM-based FEM turned out to be a useful feature. Nevertheless, the developments in this area are very recent and need further investigations to exploit their full potential.

Acknowledgements The Author would like to thank L. Beirão da Veiga and G. Manzini for providing the initial meshes used in the numerical tests.

REFERENCES

[1] P. F. Antonietti, L. Beirão da Veiga, C. Lovadina, and M. Verani. Hierarchical a posteriori error estimators for the mimetic discretization of elliptic problems. *SIAM J. Numer. Anal.*, 51(1):654–675, 2013.

[2] L. Beirão da Veiga, F. Brezzi, A. Cangiani, G. Manzini, L. D. Marini, and A. Russo. Basic principles of virtual element methods. *Math. Models Methods Appl. Sci.*, 23(01):199–214, 2013.

[3] L. Beirão da Veiga, K. Lipnikov, and G. Manzini. Arbitrary-order nodal mimetic discretizations of elliptic problems on polygonal meshes. *SIAM J. Numer. Anal.*, 49(5):1737–1760, 2011.

[4] L. Beirão da Veiga and G. Manzini. Residual *a posteriori* error estimation for the virtual element method for elliptic problems. *ESAIM Math. Model. Numer. Anal.*, 49(2):577–599, 2015.

[5] L. Chen, J. Wang, and X. Ye. A posteriori error estimates for weak Galerkin finite element methods for second order elliptic problems. *J. Sci. Comput.*, 59(2):496–511, 2014.

[6] D. Copeland, U. Langer, and D. Pusch. From the boundary element domain decomposition methods to local Trefftz finite element methods on polyhedral meshes. In *Domain decomposition methods in science and engineering XVIII*, volume 70 of *Lect. Notes Comput. Sci. Eng.*, pages 315–322. Springer, Berlin Heidelberg, 2009.

[7] V. Dolejší, M. Feistauer, and V. Sobotíková. Analysis of the discontinuous Galerkin method for nonlinear convection-diffusion problems. *Comput. Methods Appl. Mech. Engrg.*, 194(25-26):2709–2733, 2005.

[8] W. Dörfler. A convergent adaptive algorithm for Poisson's equation. *SIAM J. Numer. Anal.*, 33(3):1106–1124, 1996.

[9] Y. Efendiev, J. Galvis, R. Lazarov, and S. Weißer. Mixed FEM for second order elliptic problems on polygonal meshes with BEM-based spaces. In I. Lirkov, S. Margenov, and J. Waśniewski, editors, *Large-Scale Scientific Computing*, Lecture Notes in Computer Science, pages 331–338. Springer, Berlin Heidelberg, 2014.

[10] C. Hofreither, U. Langer, and S. Weißer. Convection adapted BEM-based FEM. *ArXiv e-prints*, 2015. arXiv:1502.05954.

[11] O. A. Karakashian and F. Pascal. A posteriori error estimates for a discontinuous Galerkin approximation of second-order elliptic problems. *SIAM J. Numer. Anal.*, 41(6):2374–2399 (electronic), 2003.

[12] W. C. H. McLean. *Strongly elliptic systems and boundary integral equations*. Cambridge University Press, Cambridge, 2000.

[13] S. Rjasanow and S. Weißer. Higher order BEM-based FEM on polygonal meshes. *SIAM J. Numer. Anal.*, 50(5):2357–2378, 2012.

[14] S. Rjasanow and S. Weißer. FEM with Trefftz trial functions on polyhedral elements. *J. Comput. Appl. Math.*, 263:202–217, 2014.

[15] O. Steinbach. *Numerical approximation methods for elliptic boundary value problems: finite and boundary elements*. Springer, New York, 2007.

[16] R. Verfürth. *A posteriori error estimation techniques for finite element methods*. Numerical Mathematics and Scientific Computation. Oxford University Press, Oxford, 2013.

[17] J. Wang and X. Ye. A weak Galerkin mixed finite element method for second order elliptic problems. *Math. Comp.*, 83(289):2101–2126, 2014.

[18] S. Weißer. Residual error estimate for BEM-based FEM on polygonal meshes. *Numer. Math.*, 118(4):765–788, 2011.

[19] S. Weißer. *Finite Element Methods with local Trefftz trial functions*. PhD thesis, Universität des Saarlandes, Saarbrücken, Germany, September 2012.

[20] S. Weißer. Arbitrary order Trefftz-like basis functions on polygonal meshes and realization in BEM-based FEM. *Comput. Math. Appl.*, 67(7):1390–1406, 2014.

[21] S. Weißer. BEM-based finite element method with prospects to time dependent problems. In E. Oñate, J. Oliver, and A. Huerta, editors, *Proceedings of the jointly organized WCCM XI, ECCM V, ECFD VI, Barcelona, Spain, July 2014*, pages 4420–4427. International Center for Numerical Methods in Engineeering (CIMNE), 2014.

[22] S. Weißer. Residual based error estimate and quasi-interpolation on polygonal meshes for high order BEM-based FEM. *ArXiv e-prints*, 2015. arXiv:1511.08993.

[23] S. Weißer. Residual Based Error Estimate for Higher Order Trefftz-Like Trial Functions on Adaptively Refined Polygonal Meshes. In A. Abdulle, S. Deparis, D. Kressner, F. Nobile, and M. Picasso, editors, *Numerical Mathematics and Advanced Applications - ENUMATH 2013*, volume 103 of *Lecture Notes in Computational Science and Engineering*, pages 233–241. Springer International Publishing, 2015.